



# Suprasellar Meningioma Classification: Endoscopic Transnasal Perspective

Abdulrazag Ajan<sup>1</sup> Basim Noor Elahi<sup>1,2</sup> Saif Almeshari<sup>1</sup> Sarah Basindwah<sup>1</sup>  
Fatimah Abdulrahim Alghabban<sup>3</sup> Saud Alromaih<sup>4</sup> Ahmad Alroqi<sup>4</sup> Abdulaziz S. Alrasheed<sup>4,5</sup>  
Ashwag Alqurashi<sup>1</sup> Saad Alsaleh<sup>4</sup>

<sup>1</sup> Division of Neurosurgery, Surgery Department, College of Medicine, King Saud University, Riyadh, Saudi Arabia

<sup>2</sup> Division of Neurosurgery, Surgery Department, Security Forces Hospital, Riyadh, Saudi Arabia

<sup>3</sup> Department of Neurosurgery, King Abdulaziz Specialist Hospital, Taif, Saudi Arabia

<sup>4</sup> Department of Otorhinolaryngology – Head & Neck Surgery, College of Medicine, King Saud University, Riyadh, Saudi Arabia

<sup>5</sup> Department of Otorhinolaryngology – Head & Neck Surgery, The James Cancer Hospital, Wexner Medical Center, The Ohio State University, Columbus, Ohio, United States

Address for correspondence Basim Noor Elahi, MD, Division of Neurosurgery, Surgery Department, Security Force Hospital, Riyadh, Saudi Arabia (e-mail: Basemelahi@gmail.com).

J Neurol Surg B Skull Base 2024;85:397–405.

## Abstract

**Objectives** Midline suprasellar meningiomas include planum sphenoidale, tuberculum sellae, and diaphragma sellae meningiomas. Multiple classifications have been previously documented; however, they come with controversies and limitations, including those with surgical implications. The aim of this study was to classify suprasellar meningiomas based on their behavior toward the underlying bone and neurovascular structures.

**Methods** Patients with newly diagnosed suprasellar meningiomas that underwent extended endoscopic transnasal approach between 2015 and 2021 were included in this study. The following parameters were evaluated: chiasmatic sulcus length, location of the optic chiasm and nerves, optic canal involvement, and vascular displacement.

**Results** We identified 40 cases of midline suprasellar meningiomas, 1 diaphragma sellae meningioma (type A), 10 tuberculum sellae meningiomas (type B), 9 chiasmatic sulcus meningiomas (type C), and 10 planum sphenoidale meningiomas (type D). Asymmetrical visual complaints were most common in chiasmatic sulcus meningiomas, followed by tuberculum sellae meningiomas (66 and 50%, respectively). Chiasmatic sulcus meningiomas showed increased separation between the optic chiasm and the A1/A2 complex (8.9 mm) compared with tuberculum sellae (2.7 mm) and planum sphenoidale (1.9 mm) meningiomas. Compared with other types, increased chiasmatic sulcus length was observed in chiasmatic sulcus meningiomas.

**Conclusion** Preoperative evaluation of bone involvement and tumor relation to neurovascular structures can be used to classify suprasellar meningiomas. Chiasmatic

## Keywords

- ▶ meningioma
- ▶ suprasellar
- ▶ chiasmatic sulcus

received  
November 11, 2022  
accepted after revision  
March 27, 2023  
accepted manuscript online  
April 11, 2023  
article published online  
May 24, 2023

DOI <https://doi.org/10.1055/a-2070-8496>.  
ISSN 2193-6331.

© 2023. The Author(s).

This is an open access article published by Thieme under the terms of the Creative Commons Attribution-NonDerivative-NonCommercial-License, permitting copying and reproduction so long as the original work is given appropriate credit. Contents may not be used for commercial purposes, or adapted, remixed, transformed or built upon. (<https://creativecommons.org/licenses/by-nc-nd/4.0/>)

Georg Thieme Verlag KG, Rüdigerstraße 14, 70469 Stuttgart, Germany

sulcus meningioma is a distinct subtype of suprasellar meningiomas. Its unique behavior toward nearby neurovascular structures could be of surgical value during tumor resection.

## Introduction

Anterior skull base meningiomas account for 40% of all intracranial meningiomas. Half of these meningiomas are sphenoid wing meningiomas, including a subcategory named anterior clinoid meningiomas.<sup>1</sup> Among anterior skull base meningiomas, 15% are midline suprasellar meningiomas, which start very anteriorly as olfactory groove meningiomas, followed by planum sphenoidale, tuberculum sellae, and, most posteriorly, diaphragma sellae meningiomas.

Most midline suprasellar meningiomas affect vision. These types of meningiomas show rapid and worse visual deterioration before reaching a size that may affect the intracranial pressure. This rapid deterioration is attributed to compression of the optic chiasm and/or extension of the tumor toward the optic canal, and compression of the optic nerves within the narrow canal, which may cause acute or subacute blindness.<sup>2,3</sup>

Multiple attempts have been made to classify suprasellar meningiomas. These classifications were based on the patency of the anterior intercavernous sinus, bone expansion, and involvement of diaphragma sellae. Recently, different ratios and tumor extension parameters have also been used to distinguish suprasellar meningiomas, but no clinical significance was ascertained.<sup>4,5</sup> In the past few years, we have encountered an increasing number of cases that did not fit these classifications. In addition, obtaining bony measurements and preoperative ratios is difficult. Therefore, we aimed to classify suprasellar meningiomas based on their site of origin and behaviors toward the underlying bone and neurovascular structure displacement.

## Methods

Data from suprasellar meningiomas that were operated using the extended endoscopic transnasal approach (EETA) between 2015 and 2021 were collected. Electronic files and images were reviewed for all the cases. All newly diagnosed cases of midline suprasellar meningioma were included. Parasellar meningiomas and cases with a history of complete or partial resection through craniotomy that underwent a second surgery through EETA were excluded. Additionally, olfactory groove meningiomas were excluded from the data because of their remote location in the optic chiasm.

Demographic data including age, sex, and presenting symptoms were collected. Visual affection was analyzed as unilateral, bilateral, symmetrical, asymmetrical, and duration of visual complaints. Hormonal assessments were reviewed as well.

Preoperative images were reviewed, and computed tomography (CT) thin-cut scans were evaluated for a detailed

bony anatomy of the area (►Fig. 1A, C). The planum sphenoidale was identified as the flat area posterior to the cribriform plate and crista galli. The chiasmatic sulcus is the groove posterior to the planum sphenoidale that houses the optic chiasm. Tuberculum sellae was defined as the most posterior ridge of the anterior wall of the sellae. The diaphragma sella constitute the two dura leaves that extend from the tuberculum sella over the sella turcica to the dorsum sellae. In midsagittal CT scans of the bone window, the distance from the tuberculum sellae to the most posterior bony ridge of the planum sphenoidale was measured in millimeters and defined as sulcal length or the length of the chiasmatic sulcus (►Fig. 2C).

Magnetic resonance images were used to evaluate the mode of neurovascular structural displacement, and T2-weighted images were used to evaluate the visual apparatus displacement. Optic chiasm displacement was assessed as posteriorly displaced, superiorly displaced, or separated from the A1/A2 complex with posterior displacement (►Fig. 2A). Optic nerve locations were assessed as well (►Fig. 2B). The A1/A2 complex location was assessed on T1-weighted contrast images and evaluated in relation to the tumor superiorly or posteriorly. Moreover, the separation between the optic chiasm and the A1/A2 complex was evaluated, and the distance from the A1/A2 complex to the most anterior edge of the chiasm was measured (►Fig. 2A). T1-weighted contrast images in the coronal plane were used to evaluate the extent of the tumor through the optic nerve canal in relation to the optic nerve (►Fig. 2D, E).

The location of the chiasm and tumor extension through the canal was confirmed intraoperatively. The presence of an arachnoid layer between the neurovascular structures and tumor was also observed.

## Results

We identified 40 cases of midline suprasellar meningiomas, 1 diaphragma sellae meningioma (type A), 10 tuberculum sellae meningiomas (type B), 9 chiasmatic sulcus meningiomas (type C), and 10 planum sphenoidale meningiomas (type D). Five patients with small para-midline tumors were excluded from the analysis. Five patients had olfactory groove meningioma (►Table 1).

Suprasellar meningiomas mainly affect middle-aged females, with an average age at presentation of ~44 years (median: 45; range: 25–63). The main presenting symptoms were visual disturbances and headache (►Table 2). Bilateral symmetrical visual affection was common among planum sphenoidale meningiomas (40%), whereas asymmetric visual deterioration and unilateral visual affection were more common in tuberculum sellae meningiomas (50 and 30%,

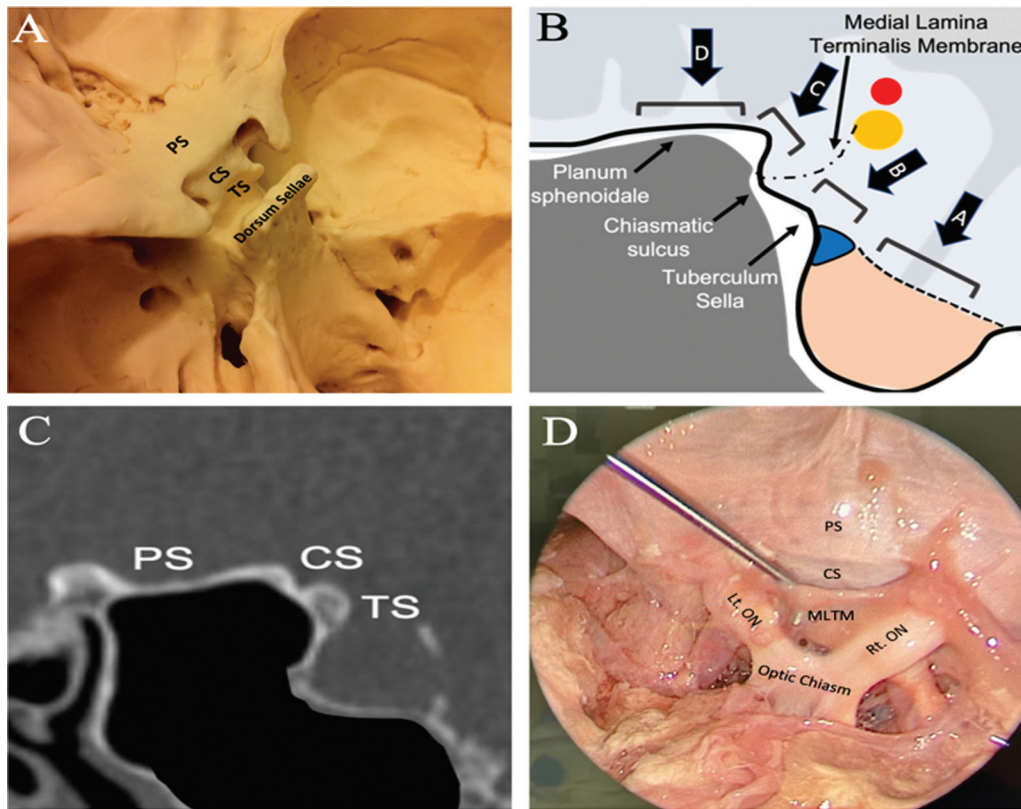


**Fig. 1** Suprasellar anatomy. (A) Superolateral view of suprasellar area showing anatomical bony landmarks. (B) Midsagittal diagrammatic illustration of the sella and suprasellar areas showing the bony landmark, the new classification of suprasellar meningioma, and the arachnoid layer medial lamina terminalis membrane. (C) CT midsagittal view of sella and suprasellar area showing the anatomical bony landmark. (D) A superior view of cadaveric dissection at suprasellar area identifying the arachnoid layer medial lamina terminalis membrane and its attachments with optic nerves and chiasm. CS: chiasmatic sulcus; Lt: left; MLTM: medial lamina terminalis membrane; ON: optic nerve; PS: planum sphenoidale; Rt: right; TS: tuberculum sella.

respectively) and chiasmatic sulcus meningiomas (44 and 55%, respectively). We had only one case of diaphragma sellae meningioma, which showed bilateral symmetrical visual affection. The duration of symptoms was the shortest in diaphragma sellae meningiomas, followed by chiasmatic sulcus, tuberculum sellae, and, lastly, planum sphenoidale (5, 9, 14, and 29 months, respectively) (– **Table 3**).

In all types, the neurovascular structure was displaced together in the same direction: superiorly in diaphragma sellae meningiomas, posteriorly and superiorly in tuberculum sellae meningiomas, and posteriorly and inferiorly in planum sphenoidale. However, in chiasmatic sulcus meningiomas, the neurovascular structure was separated from each other and displaced in a different direction, leaving the optic chiasm posterior to the tumor and the A1/A2 complex superior to it. Moreover, the sulcal length was preserved within its normal limit in all types, except for chiasmatic sulcus meningiomas, where it was enlarged in all cases with an average length of 8.5 mm (– **Table 4**).

## Discussion

The suprasellar area harbors different anatomical bony landmarks. Anterior midline suprasellar meningiomas were previously classified into three types. Type A: true tuberculum

sellae meningiomas, which displace neurovascular structures together posteriorly; type B: tuberculum-diaphragma sellae meningiomas, which displace neurovascular structures superiorly and posteriorly; and type C: true diaphragma sellae meningiomas, which displace neurovascular structures superiorly. These classifications were based on the patency of the anterior intercavernous sinus, bone expansion, and involvement of the diaphragma sellae.<sup>4</sup> Recently, another attempt to differentiate between planum sphenoidale, and tuberculum sellae meningioma was published based on the tumor distribution and extension anterior to the tuberculum sellae; this study concluded the distinction between planum sphenoidale and tuberculum sella meningioma is less useful in terms of outcomes.<sup>5</sup>

In our study, we propose a new classification system that divides these meningiomas into four types: diaphragma sellae (type A), tuberculum sellae (type B), chiasmatic sulcus (type C), and planum sphenoidale meningiomas (type D) (– **Fig. 1B**). The chiasmatic sulcus houses the optic chiasm and has direct communication with both optic canals laterally. Meningiomas in these locations exhibit different behaviors in the surrounding neurovascular structure and underlying bone. They usually present with visual deterioration followed by headaches as the main complaint.

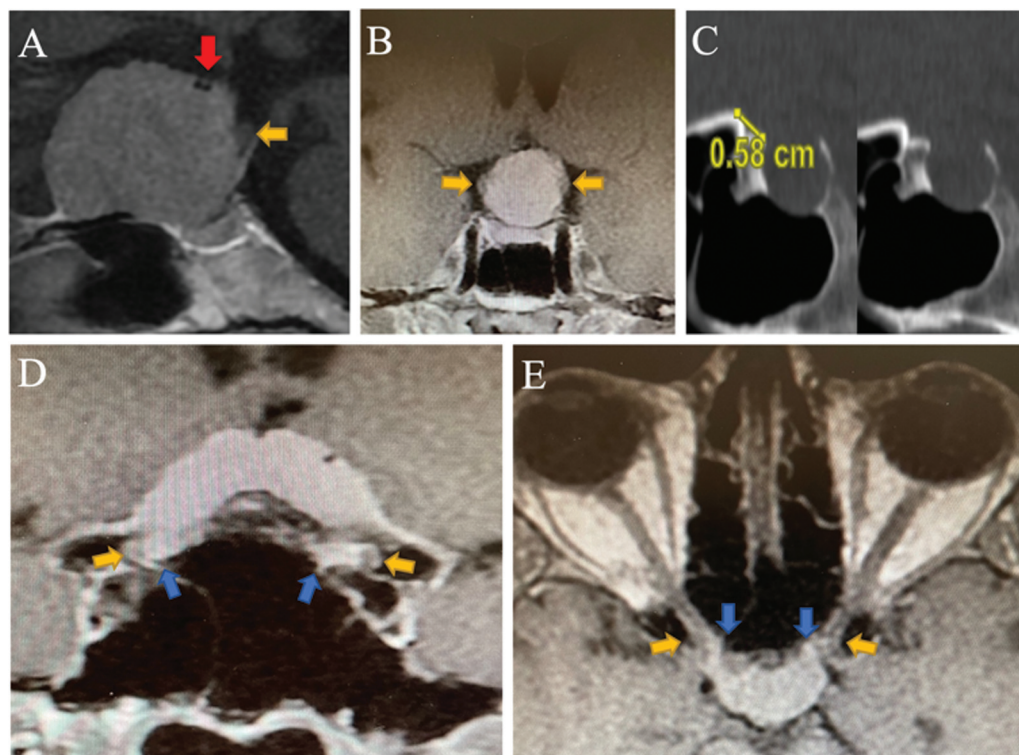


**Fig. 2** (A) Magnetic resonance imaging (MRI) T1 with contrast, sagittal view, demonstrates the displacement and separation of optic chiasm posteriorly (yellow arrow) and A1/A2 complex superiorly (red arrow). (B) MRI T1 with contrast images: coronal view demonstrates the displacement of both optic nerves lateral (yellow arrows). (C) CT sagittal view bone window showing the measurement method for sulcal length. (D) MRI T1 with contrast, coronal view and (E) MRI T1 with contrast, axial view, both demonstrating the extension of the tumor through optic canal (blue arrows) medial to the optic nerves (yellow arrows).

**Table 1** Number of cases for each type

Type	A	B	C	D
Number <sup>a</sup>	1	10	9	10

<sup>a</sup>Five cases were para-midline suprasellar meningioma; five cases were olfactory groove meningioma.

**Table 2** Demographic data

Age, y	Median: 45 Range: 25–63
Sex	F: 24, M: 3 F:M ratio: 8:1
Presenting symptoms	Visual complains: 70% Headache: 50% Hormonal disturbances: 30%

In our series, we had one case of a diaphragma sellae meningioma (type A), which displaced the neurovascular structure superiorly together. This patient presented with asymmetric visual deterioration, with poor vision on the side where the tumor extended to the optic canal. This meningioma preserved the sulcal length within the normal range (<7.45 mm) (►Fig. 3A–D).<sup>6</sup>

Tuberculum sellae meningiomas (type B) were the most common type of meningioma in this study (10 cases). In all cases that fit this category, the neurovascular structure was displaced together superiorly and posteriorly to the tumor; the sulcal length was preserved below 7.45 mm, and predominantly presented with asymmetric visual deterioration or unilateral visual deterioration (►Fig. 3E–H).

Chiasmatic sulcus meningiomas (type C) showed unique behaviors toward the surrounding structure; it displaced the neurovascular structure and separated the optic chiasm posteriorly and the A1/A2 complex superiorly to the tumor with a median distance of ~8.9 mm (►Fig. 4C). This observation can be attributed to the presence of an arachnoid layer that protects the optic chiasm and optic nerves but does not cover the A1/A2 complexes; this was observed intraoperatively (►Fig. 3I–L).

Kurucz et al performed an anatomic study that supports this observation. They named this layer the medial lamina terminalis membrane (MLTM).<sup>7</sup> This layer was indirectly illustrated by Yasargil, as he described the chiasmatic cistern as a space.<sup>8</sup> The superior boundary of the chiasmatic cistern matches the description made by Kurucz et al for MLTM. We dissected two fresh cadaveric heads to examine this layer (►Fig. 1D). This layer is a midline arachnoid layer that extends from the posterior edge of both gyri recti, covering both optic nerves and chiasm without protecting the A1/A2

**Table 3** Visual symptoms and duration and optic canalicular extension

Types	Visual complaints	Duration of symptoms (mo)	Canal extension
A: Diaphragma sella meningioma	Asymmetrical: (100%)	5	Inferior
B: Tuberculum sella meningiomas	Bilateral symmetrical: (10%) Unilateral: (40%) Asymmetrical: (50%) Not affected: (0.0%)	12	Medial
C: Chiasmatic sulcus meningiomas	Bilateral symmetrical: (0.0%) Unilateral: (33%) Asymmetrical: (66%) Not affected: (0.0%)	10	Medial
D: Planum sphenoidale meningiomas	Bilateral symmetrical: (40%) Unilateral: (20%) Asymmetrical: (20%) Not affected: (20%)	29	Superomedial

**Table 4** Behavior toward surrounding structures

Types	Sulcal length (average)	Optic chiasm displacement	A1/A2 complex displacement	Neurovascular distance (median)
A: Diaphragma sella meningioma	5.9 mm	Superior	Superior	2 mm
B: Tuberculum sella meningiomas	5.2 mm	Posterior and superior	Posterior and superior	2.7 mm
C: Chiasmatic sulcus meningiomas	8.5 mm	Posterior	Superior	8.9 mm
D: Planum sphenoidale meningiomas	6.125 mm	Inferior	Inferior	1.9 mm

complex, and it is attached anteriorly to the tuberculum sellae. The A1/A2 complex is covered with a different layer, as Yasargil mentioned in his study on anterior cerebral arteries that define the lamina terminalis cistern; its anteroinferior limit is the superior surface of the optic chiasm.<sup>7,8</sup>

During endoscopic resection of suprasellar meningiomas, the MLTM acted as a protective layer for the optic chiasm, and its location varies and can be predicted once the type of meningioma is identified. This layer covered meningiomas that arose from underneath its level, as seen in diaphragma sella and tuberculum sella meningiomas (►Fig. 3A, E). Moreover, we intraoperatively observed this after removing the tumor of type B tuberculum sellae meningiomas (►Fig. 5D), while in types C and D, it was below the tumor and extended, protecting the chiasm (►Fig. 3I, M). This observation was also observed intraoperatively, as depicted in ►Fig. 4D, E and ►Fig. 6D, E, which could be a useful intraoperative step in deciding where to start the dissection, aiming to maintain an intact layer to protect the chiasm and minimize chiasm manipulation.

In reviewing the operative notes, the A1/A2 complex was found to be protected by the arachnoid membrane in all types, except type C (chiasmatic sulcus meningiomas).

In contrast to other types of meningiomas, the sulcal length was enlarged in all cases, with an average length of 8.5 mm (►Fig. 5A).<sup>6</sup> Chiasmatic sulcus meningiomas shared the main presenting complaint with other types of meningiomas, as visual deteriorations were the main presenting

complaints, and were mainly asymmetric visual deteriorations followed by unilateral visual affection.

In planum sphenoidale meningiomas (type D), the neurovascular structure was displaced together, inferiorly to the tumor. The sulcal length was within normal limits. Cases of this type commonly presented with bilaterally symmetric visual deterioration (►Fig. 3M–P).

Patients with suprasellar meningiomas, specifically types A, B, and C, usually present with symptoms more rapidly than other meningioma locations and benign slow-growing pathologies (craniopharyngioma or hypothalamic optic pathway gliomas). Despite the relatively short period of complaints for slow-growing lesions, patients often present with severe visual loss, in which urgent intervention is needed. They usually present with unilateral visual deterioration with almost-normal vision or disproportionately mild vision loss on the other side; this supports unilateral canal compression rather than midline optic chiasm compression and displacement. Likewise, symptoms of high intracranial pressure or hormonal imbalance are usually uncommon presentations of these types of meningiomas. In our study, the average time spans from initial symptoms to diagnosis were 5, 12, and 10 months, respectively. As expected, planum sphenoidale meningiomas (type D) had a longer time from presenting symptoms to seeking medical attention (29 months). This difference in the presentation period can be attributed to the proximity of these locations to the optic canal and visual apparatus.

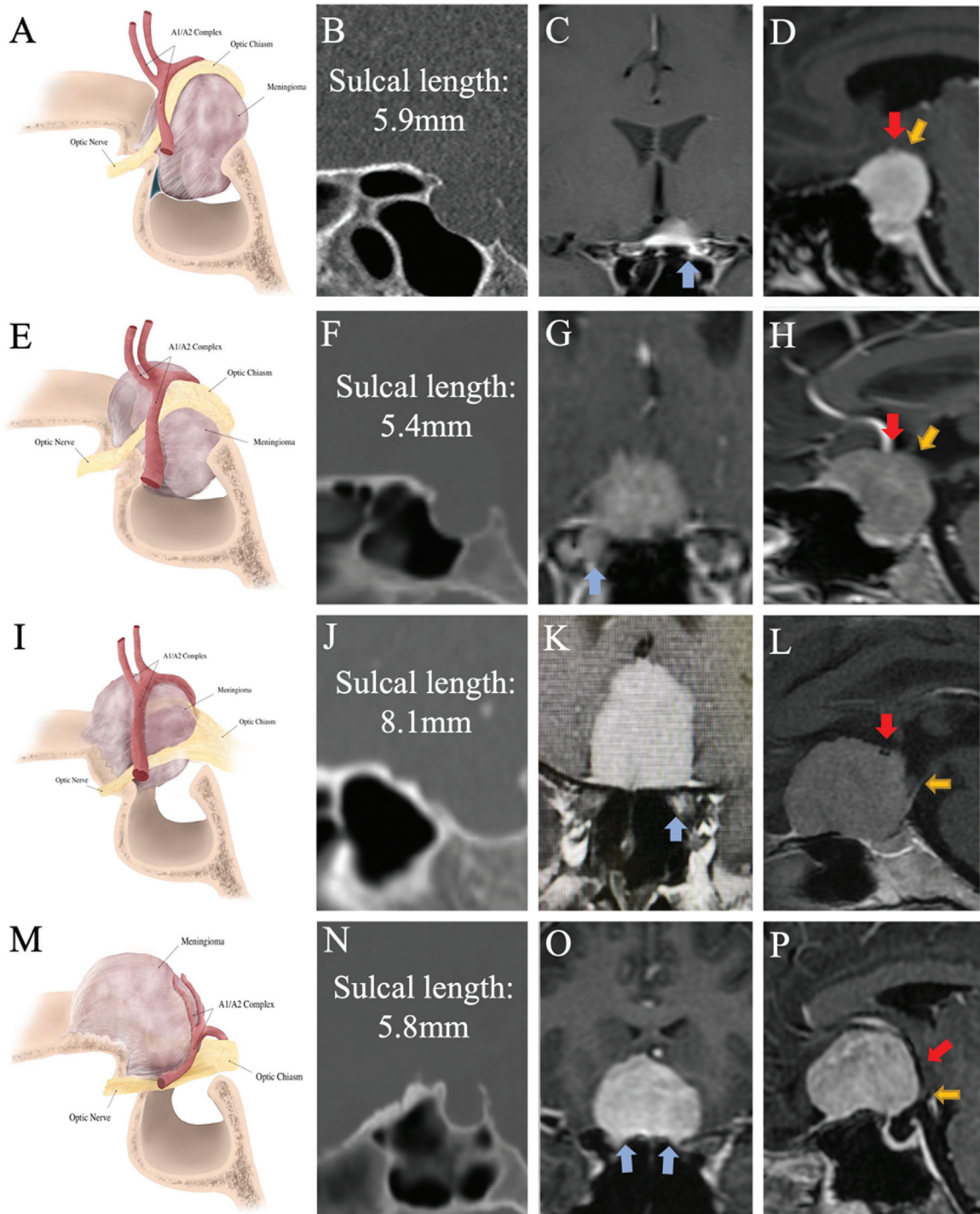


**Fig. 3** Diagram and radiological illustration of suprasellar meningiomas subtypes: Type A diaphragma sellae meningioma: (A) diagram illustration of type A diaphragma sellae meningioma, (B) CT scan sagittal view showing the sulcal length, (C) MRI with contrast coronal view showing tumor extension in the optic canal inferior to the optic nerve (blue arrow), (D) MRI with contrast sagittal view showing the displacement of the neurovascular structure superiorly, optic chiasm (yellow arrow) and A1/A2 complex (red arrow). Type B tuberculum sellae meningioma: (E) diagram illustration of type B tuberculum sellae meningioma, (F) CT scan sagittal view showing the sulcal length, (G) MRI with contrast coronal view showing tumor extension in the optic canal medial to the optic nerve (blue arrow), (H) MRI with contrast sagittal view showing the displacement of the neurovascular structure posteriorly and superiorly, optic chiasm (yellow arrow), and A1/A2 complex (red arrow). Type C chiasmatic sulcus meningioma: (I) diagram illustration of type C chiasmatic sulcus meningioma, (J) CT scan sagittal view showing the sulcal length, (K) MRI with contrast coronal view showing tumor extension in the optic canal medial to the optic nerve (blue arrow), (L) MRI with contrast sagittal view showing the displacement and separation of the neurovascular structure posteriorly, optic chiasm (yellow arrow), and superiorly A1/A2 complex (red arrow). Type D planum sphenoidale meningioma: (M) diagram illustration of type D planum sphenoidale meningioma, (N) CT scan sagittal view showing the sulcal length, (O) MRI with contrast coronal view showing tumor extension in the optic canal superior and medial to the optic nerve (blue arrow), (P) MRI with contrast sagittal view showing the displacement of the neurovascular structure posteriorly, optic chiasm (yellow arrow) and A1/A2 complex (red arrow).

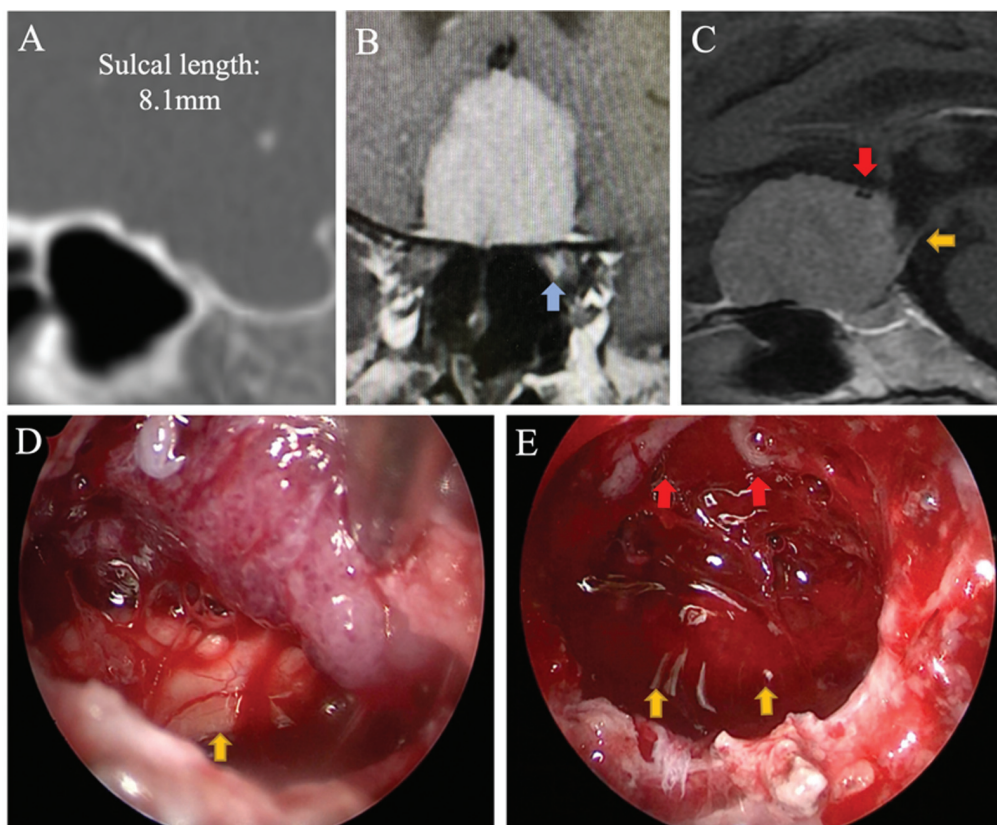


**Fig. 4** Case demonstration of type C chiasmatic sulcus meningioma. (A) CT scan sagittal view of the sellar area showing the sulcal length. (B) MRI with contrast coronal view showing tumor extension to the left optic canal (blue arrow). (C) Sagittal MRI with contrast showing the displacement and the separation of neurovascular structure posteriorly, optic chiasm (yellow arrow) and superiorly A1/A2 complex (red arrow). (D) Intraoperative picture of the arachnoid layer (medial lamina terminalis membrane) after removing the tumor as it was resting over it and protecting the optic chiasm. (E) Intraoperative picture after removing the tumor showing the separation between the optic chiasm and A1/A2 complex.

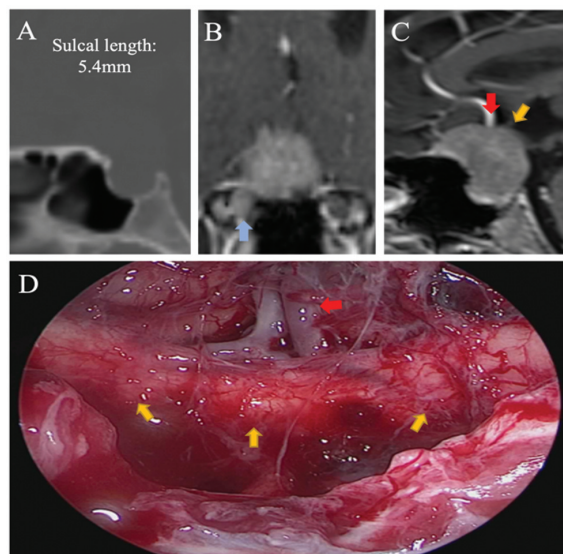


**Fig. 5** Case demonstration of type B tuberculum sellae meningioma. (A) CT scan sagittal view of the sellar area showing the sulcal length. (B) MRI with contrast coronal view showing tumor extension to the right optic canal (blue arrow). (C) Sagittal MRI with contrast showing the displacement of neurovascular structure posteriorly and superiorly, optic chiasm (yellow arrow) and A1/A2 complex (red arrow). (D) Intraoperative picture of the arachnoid layer (medial lamina terminalis membrane) after removing the tumor as it was covering the tumor and protecting the neurovascular complex.

Canal extension was closer to the affected eye. This observation explains why the main cause of visual deterioration is canal crowding and tumor extension rather than the mass effect of the tumor size and its displacement of the visual apparatus. This observation can change the main aims of treating these types of suprasellar meningiomas toward optic nerve canal decompression rather than tumor debulking and decompression of only the optic chiasm.

Types A, B, and C showed intracanalicular extension (→ Fig. 3C, G, K, O) that was medial to the optic nerve in types B and C (→ Fig. 4B and → Fig. 5B), inferior to the optic nerve in type A (→ Fig. 3C), and superomedial in type D (→ Fig. 6B). Only one patient with type C did not show canal extension to any of the optic nerve canals, whose preoperative visual assessment was normal. Moreover, one patient with type B had no canal extension, and the preoperative visual assessment was symmetrical. This observation can make gross total resection of the transcranial approach more difficult to achieve, as the relation of the extension will be hidden by the optic nerves from the superolateral transcranial approach. However, achieving a lower grade on the Simpson grading system for meningioma resection will be more difficult and carry a higher risk with optic nerve manipulation.<sup>3,9</sup> While in the endoscopic transnasal approach, both optic nerves can be decompressed with a similar degree of visualization without manipulation of the whole visual apparatus, it also faces

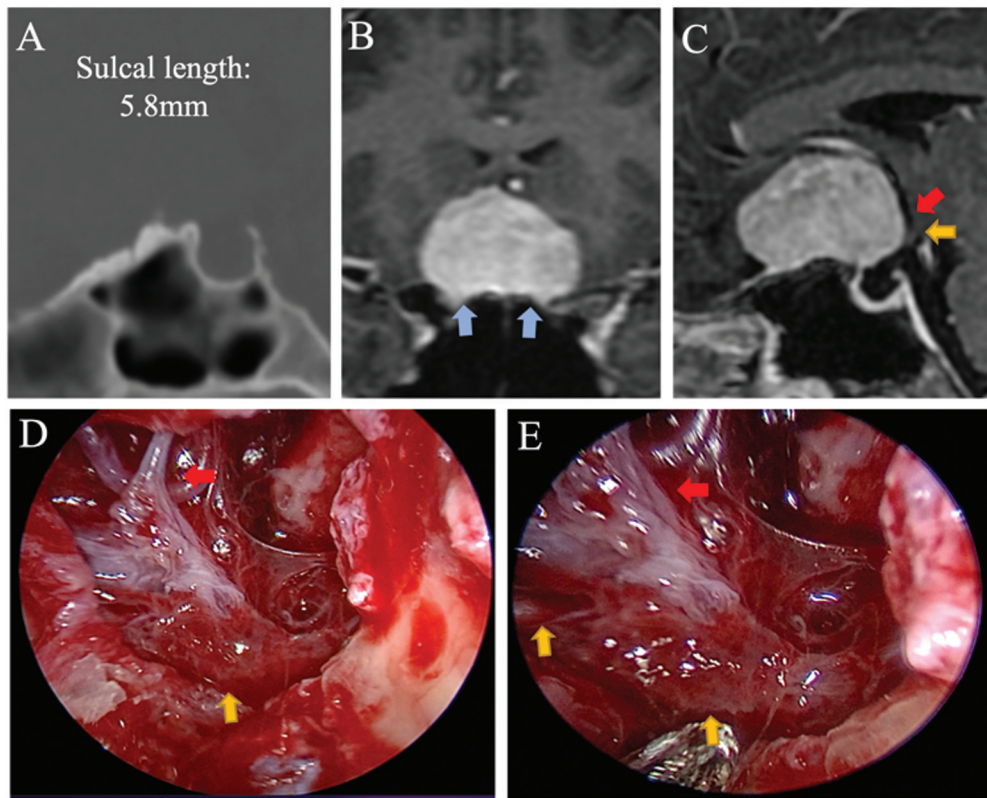


**Fig. 6** Case demonstration of type D planum sphenoidale meningioma. (A) CT scan sagittal view of the sellar area showing the sulcal length. (B) MRI with contrast coronal view showing tumor extension to both optic canals (blue arrow). (C) Sagittal MRI with contrast showing the displacement neurovascular structure posteriorly, optic chiasm (yellow arrow) and A1/A2 complex (red arrow). (D, E) Intraoperative picture of the arachnoid layer (medial lamina terminalis membrane) after removing the tumor as it was resting over it and protecting the optic chiasm.

the vascularized dura initially, which starts devascularization early in the procedure, which will facilitate tumor resection. Finally, the dura extension beyond the tumor mass can be resected safely to achieve a lower Simpson grade in endoscopic transnasal approaches.<sup>10–14</sup>

In our series, we achieved gross total resection in 86% (4/30) of the included cases. There was no statistical significance in degree of resection and major postoperative complications between the four subtypes.

Our study was limited by the small sample size and retrospective nature of the study and our proposed classification may face difficulties in classifying large tumors. Moreover, small paramedian tumors that extend to the canal before displacing the chiasm would be unsuitable for this classification.

**Conflict of Interest**  
None declared.

## References

- DeMonte F. Surgical treatment of anterior basal meningiomas. *J Neurooncol* 1996;29(03):239–248
- Al-Mefty O, Holoubi A, Rifai A, Fox JL. Microsurgical removal of suprasellar meningiomas. *Neurosurgery* 1985;16(03):364–372
- Kwancharoen R, Blitz AM, Tavares F, Caturegli P, Gallia GL, Salvatori R. Clinical features of sellar and suprasellar meningiomas. *Pituitary* 2014;17(04):342–348
- Ajlan AM, Choudhri O, Hwang P, Harsh G. Meningiomas of the tuberculum and diaphragma sellae. *J Neurol Surg B Skull Base* 2015;76(01):74–79
- Henderson F, Youngerman BE, Niogi SN, et al. Endonasal trans-sphenoidal surgery for planum sphenoidale versus tuberculum sellae meningiomas. *J Neurosurg* 2022;138(05):1338–1346
- Guthikonda B, Tobler WD Jr, Froelich SC, et al. Anatomic study of the prechiasmatic sulcus and its surgical implications. *Clin Anat* 2010;23(06):622–628
- Kurucz P, Baksa G, Patonay L, Hopf NJ. Endoscopic anatomical study of the arachnoid architecture on the base of the skull. Part I: The anterior and middle cranial fossa. *Innov Neurosurg* 2013; 1:55–66
- Yasargil MG. *Microneurosurgery*. Vol. 1. Stuttgart: George Thieme Verlag; 1996
- Mahmoud M, Nader R, Al-Mefty O. Optic canal involvement in tuberculum sellae meningiomas: influence on approach, recurrence, and visual recovery. *Neurosurgery* 2010;67(3, Suppl Operative):ons108–ons118, discussion ons118–ons119
- Fernandez-Miranda JC, Gardner PA, Snyderman CH. Endoscopic endonasal approach for tuberculum sellae meningiomas. *Neurosurgery* 2011;69(01):E260–E261
- Fernandez-Miranda JC, Pinheiro-Nieto C, Gardner PA, Snyderman CH. Endoscopic endonasal approach for a tuberculum sellae meningioma. *J Neurosurg* 2012;32(Suppl):E8



- 12 Ditzel Filho LFS, Prevedello DM, Jamshidi AO, et al. Endoscopic endonasal approach for removal of tuberculum sellae meningiomas. *Neurosurg Clin N Am* 2015;26(03):349–361
- 13 Chowdhury FH, Haque MR, Goel AH, Kawsar KA. Endoscopic endonasal extended transsphenoidal removal of tuberculum sellae meningioma (TSM): an experience of six cases. *Br J Neurosurg* 2012;26(05):692–699
- 14 Khan OH, Anand VK, Schwartz TH. Endoscopic endonasal resection of skull base meningiomas: the significance of a “cortical cuff” and brain edema compared with careful case selection and surgical experience in predicting morbidity and extent of resection. *Neurosurg Focus* 2014;37(04):E7